Biomaterials 35 (2014) 7714–7723

Contents lists available at ScienceDirect

Biomaterials

journal homepage: www.elsevier.com/locate/biomaterials

Endothelial retention and phenotype on carbonized cardiovascular implant surfaces

Christopher M. Frendl [a, 1], Scott M. Tucker [a, 1], Nadeem A. Khan [a], Mandy B. Esch [a], Shrinidhi Kanduru [a], Thong M. Cao [a], Andrés J. García [b], Michael R. King [a], Jonathan T. Butcher [a, *]

[a] Department of Biomedical Engineering, Cornell University, Ithaca, NY, USA
[b] Woodruff School of Mechanical Engineering, Georgia Institute of Technology, Atlanta, GA, USA

ARTICLE INFO

Article history:
Received 23 April 2014
Accepted 26 May 2014
Available online 20 June 2014

Keywords:
Hemodynamics
Platelet adhesion
Mechanical heart valves
Hemostasis
Computational fluid dynamics
Adhesion peptide

ABSTRACT

Heart valve disease is an increasing clinical burden for which there is no effective treatment outside of prosthetic replacement. Over the last 20 years, clinicians have increasingly preferred the use of biological prosthetics to mechanical valves despite their superior durability because of the lifelong anticoagulation therapy that is required. Mechanical valve surface engineering has largely focused on being as non-thrombogenic as possible, but despite decades of iteration has had insufficient impact on the anti-coagulation burden. In this study, we systematically evaluate the potential for endothelialization of the pyrolytic carbon surface used in mechanical valves. We compared adsorbed adhesion ligand type (collagen I, fibronectin, laminin, and purified adhesion domain fragments GFOGER and $FN_{7\text{-}10}$) and concentration on endothelial adhesion rates and adhesion strength on Medtronic-Hall prosthetic valve surfaces. Regardless of ligand type or concentration, endothelial adhesion strengthening was insufficient for their intended ultra-high shear stress environment. We then hypothesized that microfabricated trenches would reduce shear stress to tolerable levels while maintaining endothelial access to the flow stream, thereby promoting a confluent and anticoagulant endothelial monolayer. Computational fluid dynamics simulations predicted an empirical relationship of channel width, depth, and spacing that would maintain interior surface shear stress within tolerable levels. Endothelial cells seeded to confluence in these channels retained a confluent monolayer when exposed to 600 dyn/cm^2 shear stress for 48 h regardless of applied adhesive ligand. Furthermore, sheared EC expressed a mature anti-coagulant profile, including endothelial nitric oxide synthase (eNOS), VE-cadherin, and significantly downregulated plasminogen activator inhibitor-1 (PAI-1). As a final test, channeled pyrolytic carbon surfaces with confluent EC reduced human platelet adhesion 1000-fold over pyrolytic carbon alone. These results advance a promising biohybrid approach to enable active moderation of local coagulative response in mechanical heart valves, which could significantly extend the utility of this important treatment for heart valve disease.

1. Introduction

Prosthetic implantable devices remain an essential component of healthcare as the clinician's last line of defense for the treatment of serious cardiovascular disease. These devices include ventricular assist devices, total artificial hearts, mechanical heart valve replacements, and vascular stents. Each design is optimized to generate and/or maintain blood flow, which requires mechanical durability but also necessitates that the surface of the materials from which they are comprised to be in direct and continuous contact with blood. Research and clinical findings over 40 years of the so-called "first generation" of biomaterial design established that only a small set of biomaterials were suitable for implantation, including cobalt–chromium, titanium, silicone, expanded poly(-tetrafluoroethylene) (ePTFE), and some poly(ethylene) polymers [1]. The primary quality of each of these materials was that they did not elicit an inflammatory or immune response from the host. The fundamental clinical drawback from using these devices remains

* Corresponding author. Department of Biomedical Engineering, 304 Weill Hall, Cornell University, Ithaca, NY, 14850, USA. Tel.: +1 607 255 3575; fax: +1 607 255 7330.
E-mail address: jtb47@cornell.edu (J.T. Butcher).
[1] Denotes authors that contributed equally to this work.

http://dx.doi.org/10.1016/j.biomaterials.2014.05.075
0142-9612/

its hemocompatibility, or ability to function in contact with blood without inducing inappropriate clotting response. Biomaterial contact with blood can induce spontaneous coagulation through both extrinsic and intrinsic pathway cascades [2,3]. The formation of a clot can lead to local occlusion of the device, or a component can break off and occlude a distal vessel, most often leading to a stroke. As these thromboembolic events are highly unpredictable and very serious, clinicians administer anti-coagulant and anti-thrombotic cocktails to reduce these risks. Warfarin is most often prescribed for its multifaceted inhibitory properties, but anti-platelet, anti-thrombin (e.g. Dabigatran etexilate), and heparin-like molecules, and aspirin are also prescribed depending on the circumstances [4,5]. While reducing the risk of clot formation, these drugs also cause an increase in the risk of internal bleeding events, such as gastrointestinal bleeding and brain hemorrhages. Maintaining this tight balance of pro- and anti- coagulation behavior is further compounded by the fact that the coagulability of blood is dependent on the demographics and activity levels of the patient [6,7]. Despite the significant occupational and lifestyle limitations to which these patients are subjected, a 2–4% annually cumulative risk of major bleeding event is expected [8]. The superior mechanical durability of these devices, especially in the case of mechanical heart valves, has led some to propose that there would be no need for bioprosthetics if coagulation could be better controlled [1].

The first step of surface contact-induced coagulation is through platelet adhesion and activation. While hemodynamic conditions created by some devices can induce platelet activation in the blood stream, circulating platelets will readily adhere to a biomaterial surface if there are any adsorbed proteins [9]. Many attempts have been made to render prosthetic surfaces non-fouling through polymer coatings, but in vivo results to date suggest that these coatings are susceptible to cracking and wear [1,10–12]. Similarly, Milner and colleagues implemented a nano-pillar array to reduce the contact area for platelet adhesion [13]. Etching and surface texturing has also shown to modulate platelet adhesion in vitro, but results in vivo have been lacking [14,15]. Given that these devices are intended to last the rest of the patient's lifetime once implanted, it is likely impossible to ensure no protein adhesion to these surfaces with a passive process. In contrast, immobilizing anti-coagulant and/or anti-thrombotic molecules on biomaterial surfaces (e.g. thrombomodulin) has also suggested an improvement in hemocompatibility [16], but it is likely difficult to control coagulation using only one species in the cascade.

It is well known that endothelial cells, which line all natural blood contacting surfaces, are the ideal anti-coagulant and anti-thrombotic agent [17–19]. Endothelial cells secrete nitric oxide (NO), produced through the enzyme endothelial nitric oxide synthase (eNOS), which inhibits clot formation through a number of effects, including vasodilation, inhibiting the thromboxane receptor A2 (TXA2), and downregulation of adhesion receptors such as P-selectin and GPIIb-IIIa [20–22]. Endothelium also secretes tissue plasminogen activator to dissolve fibrin clots and thrombomodulin to inhibit the coagulation cascade [23,24]. Conversely, endothelium can induce clot formation as an injury response through the expression of von Willebrand Factor (vWF), Tissue Factor (TF), and/or plasminogen activator inhibitor-1 (PAI-1) [25]. Endothelial cells ensure a confluent surface layer by the formation of tight adherens junctions comprised of a number of molecules, including vascular endothelial cadherin (VE-Cad) [26]. Disruption of these junctions and/or exposure to the subendothelial tissue matrix can also induce platelet activation and aggregation. Endothelial function is directly modulated by hemodynamic signaling, namely wall shear stress, which permits natural real-time tuning of the coagulation response [27,28]. Recently, Douglas and colleagues enhanced NO production in endothelium in mice using GTP-cyclohydrolase 1 overexpression, and showed that robust healthy endothelial activity was better at reducing in-stent restenosis and clot formation than drug eluting stents regardless of strut design [29].

Endothelialization of cardiovascular biomaterial surfaces has been studied for over 30 years, most often for synthetic vascular grafts. Many studies have shown that grafts with an intact endothelial monolayer perform better and last longer than those without endothelium. Achieving confluent endothelial coverage however has been extremely challenging, in particular for long grafts where natural endothelial migration across anastomoses is of little benefit while ex vivo seeding is incomplete [30]. Strategies used to enhance endothelial coverage include enhancing bulk material porosity, surface texturing, and coating with cell adhesive peptides [31,32]. The operating range of shear stress in blood vessels is generally <50 dyn/cm^2, which suggests that once adhered an endothelial cell will not likely be detached mechanically [33]. This is not the case with mechanical prosthetic heart valves, where surface shear stresses regularly exceed 500 dyn/cm^2, far greater than what endothelium on tissue culture polystyrene can withstand (~80 dyn/cm^2) [34,35]. Only one study to date has tested whether endothelial cells could adhere to the mechanical valve surface. While a confluent monolayer was present on all the components after 1 week in culture, virtually all the cells were lost after only 1-h implantation in the mitral position of a pig [36]. The authors concluded that pyrolytic carbon was not a suitable substrate for endothelial retention under high shear stress, but no quantitative analysis was made nor complementary adhesion strategies attempted.

Recent studies have identified specific motifs on extracellular matrix ligands that increase cell adhesion strength and also modulate adherent cell phenotype [37–39]. The objective of this study therefore was to determine the effects of ligand-mediated adhesion strengthening on endothelial coverage on pyrolytic carbon surfaces exposed to fluid flow. In addition, we tested the effect of local surface shear stress reduction via microfabricated trenches on endothelial adhesion, retention under high shear stress in vitro, and hemostatic phenotype.

2. Materials and methods

2.1. Endothelial cell isolation and culture

Aortic valve endothelial cells (EC) were isolated from healthy porcine aortic valves were collagenase digestion as previously described [40, 41]. ECs were cultured in Dulbecco's Modified Eagle's Medium (Invitrogen) supplemented with 10% fetal bovine serum (Invitrogen), 3.7 g/L sodium bicarbonate (Cell Grow), 1% penicillin-streptomycin (Gibco), and 50 mg/L heparin salts (Sigma Aldrich). Cells were grown at 37 °C and 5% CO_2 and used between passage number 3 and 5.

2.2. Cell adhesion experiments

Medtronic-Hall prosthetic valve discs (25 mm diameter, kind gift from Medtronic, Inc.) were chosen because of their flat, large surface-area profile. Disc surfaces were temporarily divided into equal geometric regions with silicone isolation gaskets, and regions coated for 1 h with either type I collagen (Coll I, BD Biosciences), human fibronectin (FN, BD Biosciences), recombinant human laminin (Sigma), a recombinant fibronectin 7-10 fragment (FN_{7-10})[39, 42], or collagen-mimetic GFOGER triple helical synthetic peptide [43]at 10 μg/mL in PBS with untreated controls. This was followed by blocking of nonspecific binding with incubation in 5% nonfat dry milk in PBS for 1 h. EC were first fluorescently labeled with CellTracker RED (CTMX, Molecular Probes) according to the manufacturer's instructions. After rinsing the surfaces in PBS, 50 μL suspensions containing 10,000 labeled cells in PBS were inoculated in each well and adhesion assessed at 10, 20, 30, 40, and 50 min. Non or poorly adherent cells were dislodged by rotary shaker for 1 min at 60 rpm and then aspirated. Each region was then imaged via fluorescence microscopy and adherent cells counted via color thresholded particle image analysis using ImageJ (NIH). Next, disc regions were incubated with single proteins or peptides as above at concentrations ranging from 0.1 to 20 μg/mL in PBS for 1 h followed by blocking in 5% dry milk as before. After rinsing, similar suspensions of cells were inoculated and adhesion quantified after 10 min as before.

2.3. Cell adhesion strength measurement

A parallel plate shear bioreactor was modified from our previously described system to accommodate the Medtronic-Hall discs [44]. Briefly, discs were placed in a polycarbonate mold on top of a glass slide and the surfaces not touching the glass were surrounded with a 1% agarose gel. The system was inverted and the glass removed to reveal the pyrolytic carbon surface. This assembly was then placed inside a chamber with three separate flow domains with geometry designed to create relative wall shear stress zones of 1×, 5×, and 10×, with samples in triplicate. Shear stress was created by pulse dampened peristaltic pump (Master Flex, Cole Palmer) at flow rates of 80–320 mL/min, using different tubing sizes to achieve predicted shear stress levels from 0 to 60 dyn/cm^2. Shear stress levels in each region were verified by injection of 9.7 ± 0.4 μm polymer microspheres (Thermo Scientific) in PBS and tracking via time-lapse microscopy (Zeiss V20 stereomicroscope and Sony DXC_390 camera). Digital recordings (Streampix with pixel-linked video-converter) were converted using Virtualdub 1.6.14, velocity profiles measured by particle tracking via ImageJ, and converted into shear stress. Fluorescently labeled EC were seeded as before and subjected to 10 min of steady shear flow. Adherent cell fractions were quantified as before, and the data for each adhesion ligand converted fit to a sigmoidal curve to establish 50% adhesion strength as previously described [37].

2.4. Computational analysis of flow across surface channels

ANSYS FLUENT was used to generate 2D and 3D geometric simulations of flow over the surface of a model prosthetic heart valve with varying trench geometries. Blood was approximated as Newtonian with a viscosity of 0.0037 Pa-s and density of 1060 kg/m^3. Channel depth, width, and spacing were varied and channel surface shear stress was measured along its length (in 2D) with the objective to maintain shear stress in a stable adhesive zone based on the previous adhesion strength measurements. Flow within the chosen channel geometry was then simulated in 3D using a ¼ symmetric region of valve in an idealized open configuration under steady flow. Inlet flow rate was set at normal cardiac output of 70 mL/min. In addition, ultra-high shear flow through the bioreactor geometry was quantified using ANSYS FLUENT simulations using input flow rate specified the pump/tubing parameters, as bead tracking was not possible with imaging frame rates available. For these in vitro studies using culture media, fluid parameters were approximated as Newtonian with a viscosity of 0.00095 Pa-s and a density of 1000 kg/m^3.

2.5. Microfabrication and characterization of carbonized surface channels

As the Medtronic-Hall material was unable to be machined, we fabricated additional pyrolytic carbonized metallic surfaces. Polished silicon wafer (Silicon Quest) was cut into 1 cm^2 squares and coated with 75 nm carbon via gas evaporation (CVC SC4500 Evaporator, Cornell CNF). Regions were cut into individual samples using a dicing saw (KS 7100, Cornell CNF). Each sample was then carbon coated via gas evaporation as before. X-ray photoelectron spectroscopy (XPS, Surface Science Instruments SSX-100) was conducted at wide and narrow bands to compare the pyrolytic carbon surface chemical composition of both materials. Materials were then steam sterilized for use in experiments. As an additional confirmation of the surface characteristics, we compared the time-dependent adhesion of EC on the surface of each material, pre-coating with 10 μg/mL of fibronectin or collagen I as before.

2.6. Ultra-high shear stress testing of EC seeded micropatterned surfaces

Patterns with defined channel geometry within 1 cm^2 square regions were created and etched (Oerlikon, Cornell CNF) into a 1-mm thick silicon wafer (SVM). The channeled pyrolytic carbon surfaces were next coated with either 10 μg/mL collagen I or 10 μg/mL fibronectin for 1 h as before. EC were seeded onto the carbon surfaces at a density of 50,000 cells/cm^2 as before. The samples were then placed in the middle flow path of the bioreactor, and the other two were sealed to maximize the flow rate across the surfaces. Samples were run at maximum flow rate through the peristaltic pump for 48 h, which we previously determined approximates a chronic endothelial phenotype [41]. Cell retention over time was evaluated by CellTracker Red CMTPX labeling followed by fluorescent imaging. After 48 h shear, samples were immediately fixed in either 4%PFA or 100% methanol. Samples fixed in PFA were permeabilized with 0.2% Triton X (BD) and blocked with 1% BSA overnight at 4°C (Rockland). Samples were then incubated with primary antibodies to PECAM/CD31 (1:400, AbD Serotech), VE-Cadherin/CD144 (1:400, AbD Serotech), eNOS (1:400, BD Transduction Laboratories), and plasminogen activator inhibitor-1 (PAI-1, 1:100, Santa Cruz Biotech) overnight in 4°C. Fluorescent secondary antibodies (AlexaFluor) were then applied, in some cases with Hoechst DNA counterstain (1:10,000, Invitrogen). Samples were then imaged using a Zeiss LSM710 confocal microscope.

2.7. Human platelet adhesion tests

Blood was collected by venipuncture of healthy donors after informed consent based on Cornell Institutional Review Board (IRB) approved protocols. Human platelets were isolated from whole blood and labeled with Cell Tracker Green (Molecular Probes) as previously described [45]. Carbonized channel surfaces were pre-coated with either collagen I or fibronectin (10 μg/mL) or left uncoated. A subset of coated surfaces were also seeded with EC at a density of 50,000 cells/cm^2 as before. Samples were either cultured statically or at 600 dyn/cm^2 surface shear for 48 h. After which, samples were removed from the bioreactor, rinsed in PBS, and then exposed to freshly isolated human platelets for 1 h. Samples were then rinsed with PBS and adhered platelets quantified using ImageJ. Experiments were repeated in triplicate with platelet isolation from three different patients.

2.8. Statistics

A minimum of 6 independent experiments were conducted per condition and time point. Data was compared using Analysis of Variance followed by Tukey modified t-testing for pairwise comparisons, with $P < 0.05$ denoting significance.

3. Results

3.1. Endothelial adhesion to pyrolytic carbon

We first tested the ability of EC to adhere to the surface of the Medtronic-Hall prosthetic valve disc, and whether this could be enhanced by pre-coating with extracellular matrix proteins with specific adhesion domains. When cultured in the presence of serum-containing media, all surfaces were fully covered in seeded EC after 24 h regardless of the presence or type of ligand coating; therefore we focused subsequent experiments within the first hour of adhesion. The percentage of adherent EC increased monotonically over time regardless of ligand type, including non-coated controls, but at each time point non-coated controls contained significantly fewer adherent EC than the other ligands (Fig. 1A). We found that the rate of cell adhesion was greatest in the first 10 min for all ligands with the exception of the GFOGER peptide, which exhibited a more linear adhesion rate. Generally there was little change in relative adhesivity between ligands over time, with the exception of FN7-10, which supported the greatest adhesion at 10 min (27.5 ± 3% of original cells seeded) but only in the middle of the conditions by 50 min (41%). Analyzing this early adhesion period, we determined that the two fibronectin ligands supported greatest adhesion (50- and 36-fold greater than uncoated controls respectively, $P < 0.05$), while the two collagen ligands enhanced EC adhesion the least (25- and 13- fold greater than controls, respectively, $P < 0.05$). Interestingly, the GFOGER subunit supported less EC adhesion than the full-length collagen I, while the FN7-10 fragment supported more EC adhesion than the full-length protein. After 50 min of adhesion, however, both full-length collagen I and fibronectin supported the greatest adhesion (49.5% and 49.3% respectively), with no statistical difference between them. Laminin supported EC adhesion to a degree between collagen and fibronectin regardless of time point. Next, we determined how adhesion ligand coating concentration (an approximation of ligand density) affected EC attachment on the prosthetic surfaces. As expected, EC adhesion increased with ligand density for all ligands tested (Fig. 1C). Statistical saturation of EC adhesion with each ligand was reached at 10 μg/mL coating concentration. At this concentration, there were no statistical differences in EC adhesion for any ligand (Fig. 1D). These results demonstrate that pre-coating with adhesion ligands enhances EC adhesion in static culture, but with few differences between ligands greater than 10 μg/mL concentration and 1 h of seeding.

3.2. EC adhesion modification by protein adsorption

We next tested whether specific ligand types modify the adhesion strength of EC. We employed saturating (10 μg/mL) concentrations for each ligand, and seeded with confluent monolayers as previously described. Shear stress dependent adhesion followed sigmoidal curves with $R^2 > 0.8$ for each condition. We did not apply shear greater than 60 dyn/cm^2, as fewer than 20% of the cells

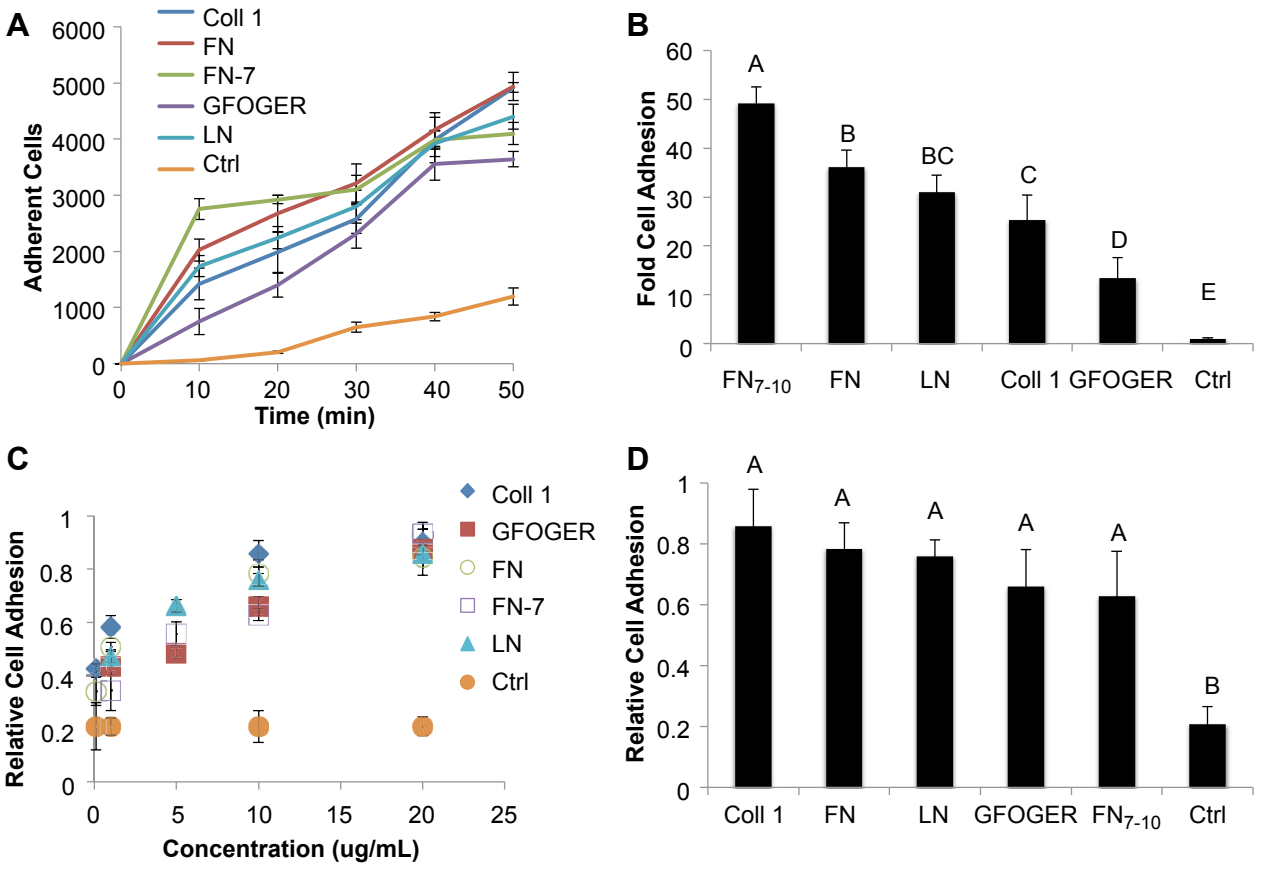

Fig. 1. Ligand dependent adhesion of endothelial cells on prosthetic mechanical valve surfaces. A) Time dependent adhesion of EC on ligand pre-coated surfaces at 10 μg/ml (10,000 cells initially seeded). B) 10 min EC adhesion comparison. C) Ligand coating concentration effect on EC adhesion (1 h). D) Comparison of EC adhesion to ECM ligand coating at 10 μg/ml (expressed relative to maximum adhesion at 1 h). Data expressed as mean ± SEM for A and C, standard deviation for B, D. For panels B and D, different letters denote significant differences.

remained adhered at this magnitude regardless of adhesion ligand. We identified significant differences in adhesion strength of EC depending on the ligand to which they were adhered (Fig. 2). Collagen I coating resulted in the highest adhesion strength (40.0 ± 1.8 dyn/cm^2), which was nearly 10-fold higher than uncoated controls (4.57 ± 1.2 dyn/cm^2, $P < 0.05$). All other ligands created EC adhesion strengths in between these values, but none significantly different from each other. These results demonstrate that EC adhesion strength is modified by adhesion ligands, but regardless of ligand, ECM coating alone will be insufficient to support an EC monolayer under high shear environments experienced for mechanical valves.

3.3. Surface microchannel design

We therefore hypothesized that surface modification to reduce wall shear stress to levels experienced on the native valve (approximately less than 70 dyn/cm^2 [46,47]) would result in increased retention of seeded EC. We first conducted CFD simulations to generate rectangular channel dimensions that would result in low shear stress. Steady input flow rates of 70 mL/min were employed for both 2D (axisymmetric) and 3D (1/4 symmetric) simulations. In 2D geometric simulations, we determined that channel width, depth, and spacing all influenced the wall shear stress. Generally, wall shear stress reduced as the channel deepened, and vortical flow developed within the channel after 200 microns in depth. A second vortex formed beyond after 500 microns in depth (Fig. 3A). For thin and shallow channels, wall shear stress was highly non-uniform particularly at the corners, but increased in homogeneity with depth and width. Furthermore, we determined that the spacing between the channel walls strongly influenced the shear stress within the walls. We identified a nonlinear relationship between channel width and spacing to maintain an average wall shear stress under 70 dyn/cm^2 (Fig. 3B). Based on this data, we chose a channel width (400 μm), depth (700 μm), and spacing (75 μm) that predicted a uniform wall shear stress of approximately 20 dyn/cm^2, which was the within the adhesion strength of the EC for all ligands tested, and also maximize the surface available for EC. We then tested this configuration in full 3D simulation. We found that 100% of the putative EC adhesion regions exhibited wall shear stresses under 70 dyn/cm^2, and approximately 90% of the surface was 25 dyn/cm^2 or less. In general, the lower range of shear stress was located at the lateral edges of each channel, while higher shear stresses were present within some of the forward channels. These results supported our hypothesis that surface channel geometry can reduce wall shear stress and thereby better retain an endothelialized surface.

3.4. Surface comparison of carbonized silicon with prosthetic valves

We deposited approximately 75 nm of carbon on to the surface of silicon using the evaporation methodology. We first analyzed compared the surface elemental composition of our carbonized silicon surfaces against that of the Medtronic-Hall prosthetic valve.

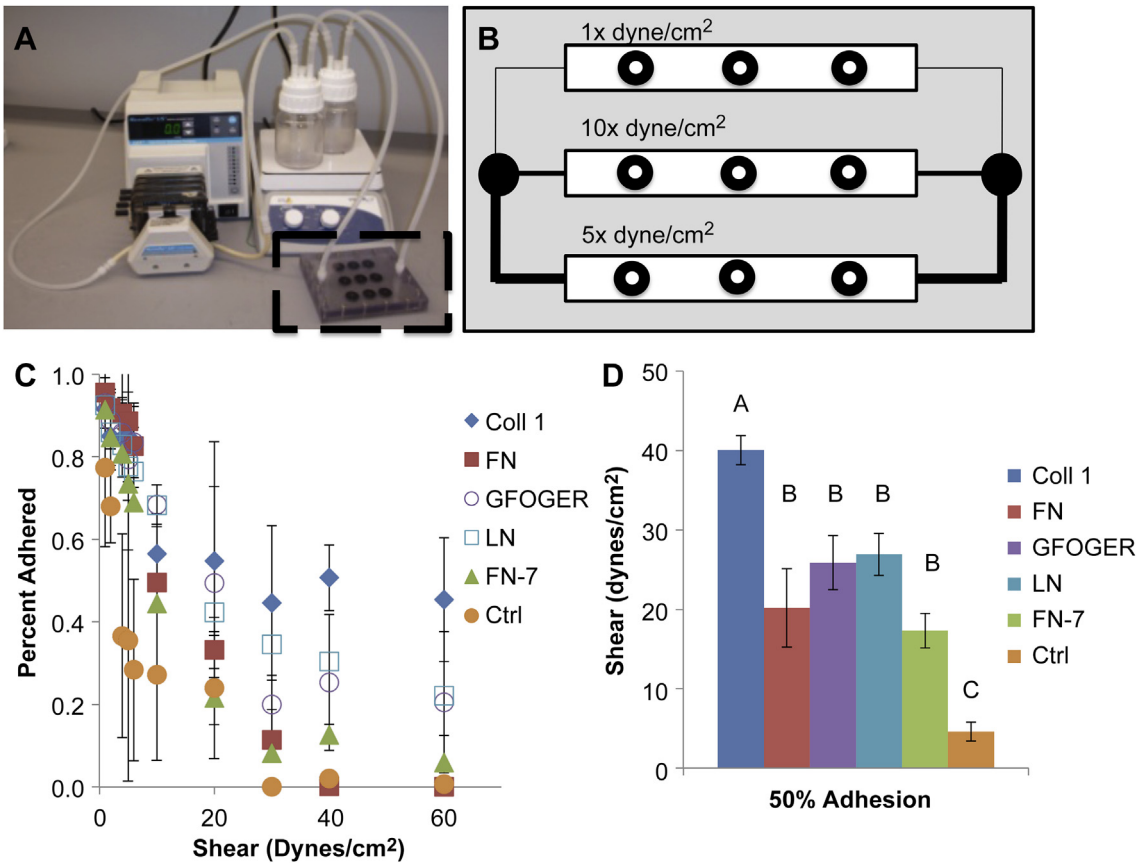

Fig. 2. Quantification of EC adhesion strength on ligand coated prosthetic valve surfaces. A) Bioreactor design. B) Schematic of the flow distribution and valve surface positions. C) Curves of endothelial retention (relative to initial seeding) after 5 min of shear stress. D) Comparison of ligand dependent EC adhesion strength, measured as shear stress at 50% detachment. Data presented as mean ± standard deviation. For panel D, different letters denote statistical significance.

We found in both cases two single identical peaks, representing oxygen and carbon, respectively (Fig. 4A). Carbon represented >90% of the surface elements, with 7.5% oxygen and trace amounts of aluminum and silicon also present. Most of the carbon was present as graphite, with some C–O bonds. The similarity between the two surfaces led us to hypothesize that they would support EC adhesion to the same degree. We compared the time dependent adhesion of EC to both surfaces coated with either fibronectin or collagen I. EC

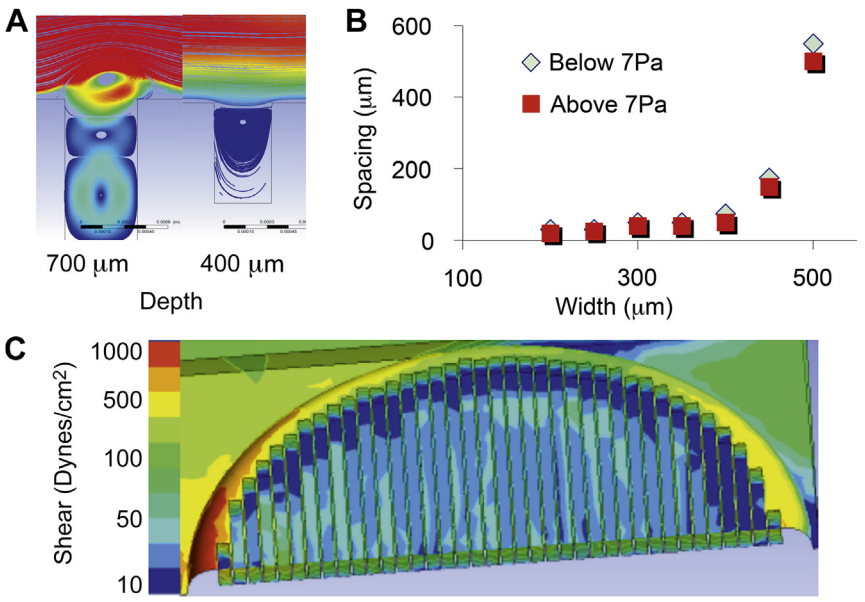

Fig. 3. Computational simulation of flow across micro-channeled surfaces. A) Effect of channel depth on blood flow patterns, B) Relationship between channel spacing and width on channel wall shear stress. C) ¼ symmetric 3D simulation of steady flow across a channeled prosthetic mechanical valve in systole.

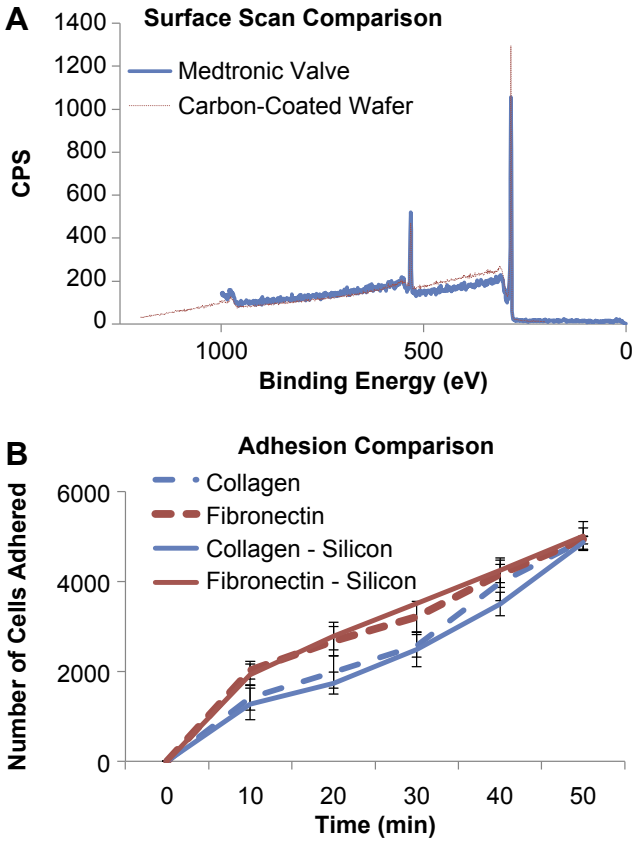

Fig. 4. Comparison of Medtronic-Hall prosthetic valve surface with pyrolytic carbon coated silicon. A) Surface atomic scan. B) Comparison of ligand dependent EC adhesion. Data expressed as mean ± standard error.

adhesion to all surface conditions increased with time, and there was no difference in adhesion between either ligand at any time point in the study (Fig. 4B). These results show that EC adhesion onto carbonized channels would approximate that on the actual valve surface.

3.5. EC adhesion and coagulant phenotype within microchannels

CFD simulations determined that the maximum flow rate employable by the pump through the middle region of the bioreactor generated a uniform shear stress of approximately 600 dyn/cm^2, which was similar to those measured with prosthetic valves in vivo and in simulations and more than 10-fold higher than the adhesive peptide-mediated EC adhesion strength (Fig. 5A). We then etched the selected channel dimensions across the full length of the 1 cm^2 surfaces. The process kept each channel cross-section rectangular (Fig. 5B). After carbon coating, and then coating with either collagen I or fibronectin, EC were seeded to confluence. We found that EC adhered not only to the base of the channels, but also the sidewalls of the channels, effectively tripling the surface area of ECs present. After EC seeding, we applied maximum surface steady shear for 48 h. Endothelial retention on the flow surface (in between the channels) was nonexistent, but we found a confluent EC monolayer was retained within the channels, with no denuded patches found (Fig. 5C). EC were also adhered along the channel walls from the surface to the base. Immunofluorescence staining determined that EC expressed tight junctions consisting of VE-cadherin (VE-Cad), and expressed endothelial nitric oxide synthase (eNOS, Fig. 5D). In static culture, EC robustly expressed plasminogen activator-inhibitor (PAI-1), a known inhibitor of fibrinolysis (Fig. 5E,F insets). After 48 h of shear however, expression was almost completely abolished. This shear reduction was not significantly different whether the surfaces were coated with collagen I or fibronectin. As a final test, we exposed sheared and static control surfaces, both with and without adhesive ligand coating and EC seeding to freshly isolated human platelets (Fig. 6). We found that platelet adhesion to bare carbon, collagen I (case 1), or fibronectin (case 2)I was extensive. While platelet adhesion to collagen I was slightly but significantly less than that of fibronectin (66.1 ± 39.8 vs. 106.5 ± 34.67 normalized counts, $P < 0.05$), neither was significantly different than bare carbon (147.5 ± 119). However, the addition of EC to the surfaces dramatically reduced the amount of platelets adhered over 100-fold (cases 3,4). No significant difference in reduction was found between collagen I or fibronectin precoating (0.36 ± 0.32 vs. 0.42 ± 0.22 normalized counts, $P > 0.05$). As hypothesized, adherent EC exposed to chronic shear stress significantly reduced platelet adhesion further still (cases 5,6), which again showed no difference between adhesive peptide coating (0.20 ± 0.11 vs. 0.14 ± 0.13 for collagen I vs. fibronectin respectively). These results confirm that endothelial cells seeded within geometrically optimized channels remain adhered within chronic ultra-high surface shear stress environments and exhibit an anticoagulant phenotype.

4. Discussion

Heart valve disease is an increasing clinical problem for which there is no biologically based treatment [48]. Prosthetic replacement will likely be the mainstay for the vast majority of patients. Approximately 80% of valve disease patients in the Western world are over the age of 70, which at current rates suggest that prosthetic valve implantation will likely outlive the patient [49]. The undesirable limitations of lifelong anticoagulation therapy has steered an increasing proportion of these patients toward biological prosthetic valves, in particular for octogenarians and older who are considered high risk for open heart surgery. Nevertheless, about 30% of these patients continue to receive mechanical valve prosthetics for their superior mechanical durability and the near certainty of a single operation for the rest of the patient's life. The situation is more muddled for middle-aged patients, who are in general more active. The superior mechanical durability of a mechanical prosthesis is likely never to be matched by a bioprosthetic, but improvements in preparation strategies for bioprosthetics have rendered risks of coagulation events nearly non-existent [50]. In general, a mechanical valve is recommended if there are any comorbidities that suggest a risk of thromboembolism (e.g. atrial fibrillation), but otherwise a bioprosthetic is preferred. Bioprosthetic valves are not suitable for children and young adults who are highly active. While the Ross procedure, or pulmonary autograft, has received significant attention over the past 20 years for the ability to provide a living conduit with growth potential for the aortic valve, results to date indicate a significant number of these neo-aortic valves will degenerate while the patient is still young, creating a dual prosthetic condition [51]. For younger patients therefore a mechanical valve is a preferred choice. Importantly, the majority world has a significant and increasing burden for valve disease, for which much larger proportion of these patients are of an age where a mechanical valve would be the valve of choice [52]. Managing anticoagulation therapy in poor medical resource environments is tremendously difficult, but these patients have little choice. Design iterations to reduce the thrombogenic burden of mechanical valves have been largely static over the past 20 years, largely because the focus was to make the surface as inert as possible. Little attention has been given to a biohybrid approach

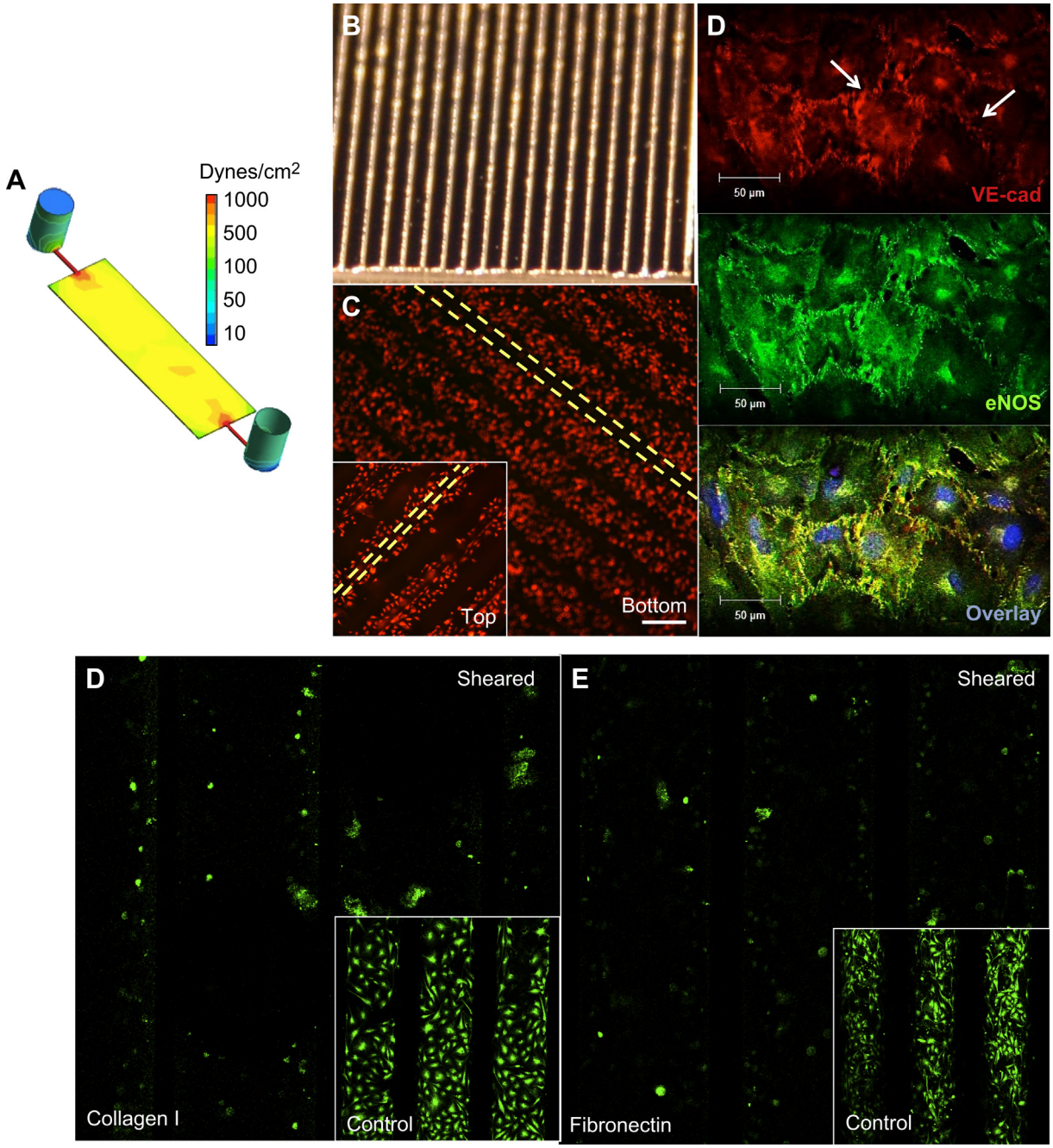

Fig. 5. Endothelial retention and phenotype under chronic ultra-high shear stress. A) CFD simulation shear stress of bioreactor channel at maximum flow. B) Etched deep channels in silicon retain rectangular profile. C) Confluent endothelial monolayers (red) are retained after 48 h of 600 dyn/cm^2 steady surface shear. Dashed line indicates surface spacing, which does not retain EC. C) 48 h Sheared EC monolayers in channels express VE-cadherin (red) and eNOS (green). D,E) Static cultured EC in channels coated with collagen I (D) or fibronectin (E) express PAI-1, which is eliminated when exposed to ultra high surface shear stress for 48 h (compare against inset). (For interpretation of the references to color in this figure legend, the reader is referred to the web version of this article.)

that could combine the natural anticoagulant and antithrombotic characteristics of endothelium with the durability of the mechanical valve. Any reduction in coagulation burden while maintaining superior mechanical durability would dramatically improve outcomes for these patients, and expand the utility of this technology.

In this study, we systematically evaluated the potential for biological ligand specific endothelialization of mechanical valve prosthetic surfaces, using both actual mechanical valve (Medtronic-Hall) discs and carbonized silicon. As expected, seeding of endothelium on bare carbon resulted in virtually no EC adhesion after 1 h, but precoating carbon surfaces with adhesion ligands does dramatically improve EC adhesion and adhesion strength. It was somewhat surprising to us that the ligand type and concentration experiments did not exhibit wider effects on EC adhesion. We and others have reported that peptides with specific adhesion motifs such as GFOGER and $FN_{7\text{-}10}$ confer greater adhesion than their full-length proteins [38,39]. Our data suggests that $FN_{7\text{-}10}$ supports most rapid EC adhesion, but GFOGER the slowest on pyrolytic carbon. After one hour, however, we found no difference in EC adhesion between ligand type, nor was there any ligand dependent difference in EC adhesion at saturating concentrations. While collagen I coating promoted strongest adhesion, no ligand type

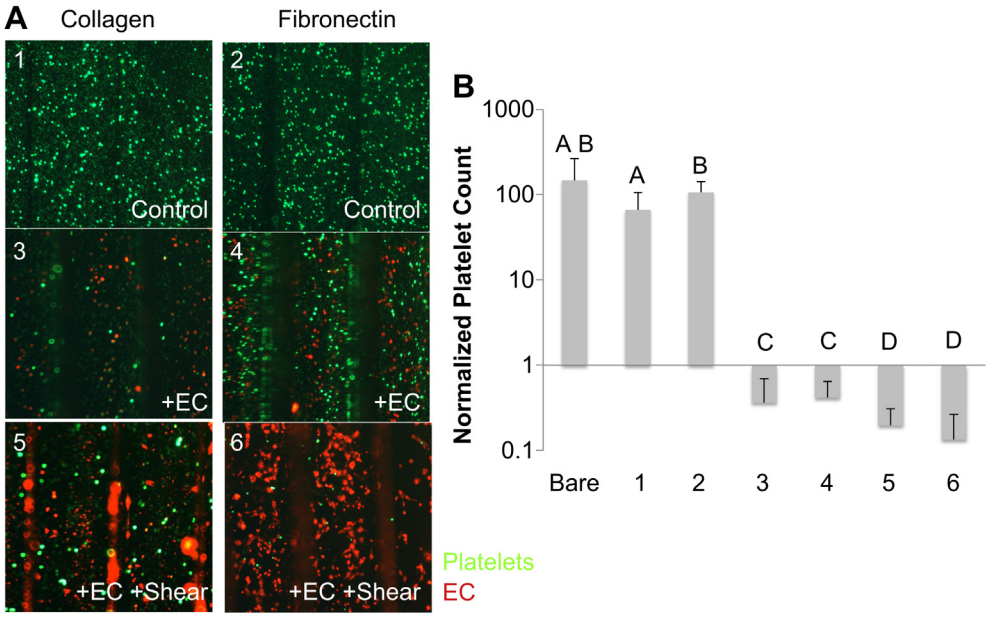

Fig. 6. Platelet adhesion to modified prosthetic surfaces. A) Images of platelets (green) and EC (red) adhered to pyrolytic carbon surfaces. Control = ECM alone. Numbers in panels indicate conditions defined by the text in lower right B) Quantification of platelet adhesion. Data presented as mean ± standard deviation. Bars not sharing letters are significantly different ($P < 0.05$). (For interpretation of the references to color in this figure legend, the reader is referred to the web version of this article.)

conferred adhesion strength sufficient for the expected environment of the prosthetic valve. Adhesion strength is influenced by many factors, including ligand type and density, but also the adsorbing surface and the type of cell involved. Endothelial cells express a variety of integrins, and are capable of binding to each of the ligands [41,53,54]. Our findings confirm and explain previous observations using EC cultured for two weeks on uncoated prosthetic valve surfaces. While EC were present in static culture, no EC remaining on the carbonized leaflets after 1-h implantation in the mitral position of a pig [36]. Two weeks culture is sufficient time for a variety of extracellular matrix ligands to be secreted [55], but no identification of these were made in their study. This result suggests that mixing pre-adsorbed ligand types would not likely provide sufficient adhesion strengthening in this context [42].

We then hypothesized that local reduction of shear stress burden on EC would retain greater numbers of EC and thereby present an anticoagulant surface in ultra-high shear stress. Some previous studies employed microfabricated wells to promote docking of circulating cells for microfluidic assays, but this method required very low shear stresses (<0.05 dyn/cm^2), and the assistance of microfluidic valves [56]. We here identified empirical relationships between channel depth, width, and spacing that would reduce surface shear stress to within physiological levels on the valve leaflet surface (<7 Pa). We therefore chose dimensions that would maximize the surface available for EC adhesion (thinnest spacing with widest channels). These optimized microfabricated trenches resulted in retention of confluent EC monolayers despite over 600 dyn/cm^2 of shear stress at the valve surface for a chronic flow period (48 h). We are unaware of any other technique published that was able to retain EC within such a demanding hemodynamic environment.

Recent studies evaluating the performance of drug eluting vascular stents have identified an increasing risk of late (>1 year post-implantation) in-stent thrombosis and neoatherosclerosis. Researchers have found that secreted anti-proliferative drugs impair endothelial coverage of the stent, and the endothelium that is present is significantly impaired in its ability to maintain normal vessel homeostasis [10]. Therefore, a complete and healthy endothelium needs to be present for therapeutic benefits to be realized and maintained long term. With our approach, we found no gaps in the endothelial retention under shear, and these EC expressed both endothelial nitric oxide synthase and VE-cadherin while almost eliminating the pro-thrombotic plasminogen activator inhibitor-1 (PAI1). Furthermore, EC coated channels exhibited near 1000-fold reduction in platelet adhesion over bare carbon. We did not detect a significant difference in platelet adhesion between coating with collagen or fibronectin. Platelets have adhesion receptors to matrix ligands including collagen I and fibronectin, and serum contains several adhesion ligands that readily adsorb to biomaterial surfaces [57,58] Together these findings suggest that maintaining a lower shear stress environment is much more important for endothelial function than the type of adhesion ligand coating.

5. Conclusions

Our results advance a technology for improving mechanical valve non-thrombogenic performance through combining a protected but accessible confluent surface endothelium. The fact that endothelial cells sense and respond in real time to hemodynamic and biochemical changes in the blood stream to maintain hemostasis supports the potential to reduce the burden of pharmacological anticoagulation management. While it is possible to recruit circulating endothelial progenitors from the blood stream, for instance using CD34 ligands, our results demonstrate that platelet adhesion is rapid and significant without a confluent endothelial monolayer present. It is unlikely that development of a confluent endothelium within these channels in vivo will be possible, and even if so the timing to achieve such a covering may not result in a sufficiently healthy endothelium for long term function, as has been reported for cardiovascular stents [59]. Our results advocate for in vitro seeding to ensure complete coverage of the valve leaflet surfaces, which can be done routinely and within 24 h of implantation. It will be critically important to test this approach in the physiological setting with the full complement of blood components and native hemodynamic stress environments, but these

mechanistic findings indicate a promising rejuvenation of an essential clinical material in our arsenal to treat cardiovascular disease.

Acknowledgments

This research was supported by grants from the National Institutes of Health (R21 HL118672 to JTB, R01 AR062920 to AJG, R01 HL097971 to MRK) and the Cornell University Engineering Learning Initiatives. This work was performed in part at the Cornell NanoScale Facility, a member of the National Nanotechnology Infrastructure Network, which is supported by the National Science Foundation (Grant ECCS-0335765). The authors have no financial conflicts to disclose.

References

[1] Williams DF. On the mechanisms of biocompatibility. Biomaterials 2008;29:2941–53.
[2] McGuigan AP, Sefton MV. The influence of biomaterials on endothelial cell thrombogenicity. Biomaterials 2007;28:2547–71.
[3] Gorbet MB, Sefton MV. Biomaterial-associated thrombosis: roles of coagulation factors, complement, platelets and leukocytes. Biomaterials 2004;25:5681–703.
[4] Hering D, Piper C, Horstkotte D. Drug insight: an overview of current anticoagulation therapy after heart valve replacement. Nat Clin Pract Cardiovasc Med 2005;2:415–22.
[5] Massel DR, Little SH. Antiplatelet and anticoagulation for patients with prosthetic heart valves. Cochrane Database Syst Rev 2013;7:CD003464.
[6] Kaneko T, Aranki SF. Anticoagulation for prosthetic valves. Thrombosis 2013;2013:346752.
[7] Heneghan C, Ward A, Perera R, Self-Monitoring Trialist C, Bankhead C, Fuller A, et al. Self-monitoring of oral anticoagulation: systematic review and meta-analysis of individual patient data. Lancet 2012;379:322–34.
[8] Grunkemeier GL, Li HH, Naftel DC, Starr A, Rahimtoola SH. Long-term performance of heart valve prostheses. Curr Probl Cardiol 2000;25:73–154.
[9] Yoshimoto Y, Hasebe T, Takahashi K, Amari M, Nagashima S, Kamijo A, et al. Ultrastructural characterization of surface-induced platelet activation on artificial materials by transmission electron microscopy. Microsc Res Tech 2013;76:342–9.
[10] Kolandaivelu K, Swaminathan R, Gibson WJ, Kolachalama VB, Nguyen-Ehrenreich KL, Giddings VL, et al. Stent thrombogenicity early in high-risk interventional settings is driven by stent design and deployment and protected by polymer-drug coatings. Circulation 2011;123:1400–9.
[11] Levy Y, Mandler D, Weinberger J, Domb AJ. Evaluation of drug-eluting stents' coating durability–clinical and regulatory implications. J Biomed Mater Res B Appl Biomater 2009;91:441–51.
[12] Otsuka Y, Chronos NA, Apkarian RP, Robinson KA. Scanning electron microscopic analysis of defects in polymer coatings of three commercially available stents: comparison of BiodivYsio, Taxus and Cypher stents. J Invasive Cardiol 2007;19:71–6.
[13] Milner KR, Snyder AJ, Siedlecki CA. Sub-micron texturing for reducing platelet adhesion to polyurethane biomaterials. J Biomed Mater Res A 2006;76:561–70.
[14] Lau KH, Ren C, Sileika TS, Park SH, Szleifer I, Messersmith PB. Surface-grafted polysarcosine as a peptoid antifouling polymer brush. Langmuir 2012;28:16099–107.
[15] Martinez AW, Chaikof EL. Microfabrication and nanotechnology in stent design. Wiley Interdiscip Rev Nanomed Nanobiotechnol 2011;3:256–68.
[16] Jordan SW, Chaikof EL. Novel thromboresistant materials. J Vasc Surg 2007;45(Suppl. A):A104–15.
[17] Otsuka F, Finn AV, Yazdani SK, Nakano M, Kolodgie FD, Virmani R. The importance of the endothelium in atherothrombosis and coronary stenting. Nat Rev Cardiol 2012;9:439–53.
[18] Wu KK, Thiagarajan P. Role of endothelium in thrombosis and hemostasis. Annu Rev Med 1996;47:315–31.
[19] Vane JR, Anggard EE, Botting RM. Regulatory functions of the vascular endothelium. N Engl J Med 1990;323:27–36.
[20] Napoli C, de Nigris F, Williams-Ignarro S, Pignalosa O, Sica V, Ignarro LJ. Nitric oxide and atherosclerosis: an update. Nitric Oxide Biol Chem/Official J Nitric Oxide Soc 2006;15:265–79.
[21] Wang GR, Zhu Y, Halushka PV, Lincoln TM, Mendelsohn ME. Mechanism of platelet inhibition by nitric oxide: in vivo phosphorylation of thromboxane receptor by cyclic GMP-dependent protein kinase. Proc Natl Acad Sci U S A 1998;95:4888–93.
[22] Li JM, Podolsky RS, Rohrer MJ, Cutler BS, Massie MT, Barnard MR, et al. Adhesion of activated platelets to venous endothelial cells is mediated via GPIIb/IIIa. J Surg Res 1996;61:543–8.
[23] Smith D, Gilbert M, Owen WG. Tissue plasminogen activator release in vivo in response to vasoactive agents. Blood 1985;66:835–9.
[24] Murata M, Ikeda Y, Araki Y, Murakami H, Sato K, Yamamoto M, et al. Inhibition by endothelial cells of platelet aggregating activity of thrombin–role of thrombomodulin. Thromb Res 1988;50:647–56.
[25] Fujii S, Sawa H, Saffitz JE, Lucore CL, Sobel BE. Induction of endothelial cell expression of the plasminogen activator inhibitor type 1 gene by thrombosis in vivo. Circulation 1992;86:2000–10.
[26] Dejana E, Tournier-Lasserve E, Weinstein BM. The control of vascular integrity by endothelial cell junctions: molecular basis and pathological implications. Dev Cell 2009;16:209–21.
[27] Ensley AE, Nerem RM, Anderson DE, Hanson SR, Hinds MT. Fluid shear stress alters the hemostatic properties of endothelial outgrowth cells. Tissue Eng Part A 2012;18:127–36.
[28] Bergh N, Larsson P, Ulfhammer E, Jern S. Effect of shear stress, statins and TNF-alpha on hemostatic genes in human endothelial cells. Biochem Biophys Res Commun 2012;420:166–71.
[29] Douglas G, Van Kampen E, Hale AB, McNeill E, Patel J, Crabtree MJ, et al. Endothelial cell repopulation after stenting determines in-stent neointima formation: effects of bare-metal vs. drug-eluting stents and genetic endothelial cell modification. Eur Heart J 2013;34:3378–88.
[30] Zilla P, Bezuidenhout D, Human P. Prosthetic vascular grafts: wrong models, wrong questions and no healing. Biomaterials 2007;28:5009–27.
[31] Meyers SR, Kenan DJ, Khoo X, Grinstaff MW. Bioactive stent surface coating that promotes endothelialization while preventing platelet adhesion. Biomacromolecules 2011;12:533–9.
[32] Lu J, Rao MP, MacDonald NC, Khang D, Webster TJ. Improved endothelial cell adhesion and proliferation on patterned titanium surfaces with rationally designed, micrometer to nanometer features. Acta Biomater 2008;4:192–201.
[33] Samijo SK, Willigers JM, Barkhuysen R, Kitslaar PJ, Reneman RS, Brands PJ, et al. Wall shear stress in the human common carotid artery as function of age and gender. Cardiovasc Res 1998;39:515–22.
[34] Woo YR, Yoganathan AP. In vitro pulsatile flow velocity and shear stress measurements in the vicinity of mechanical mitral heart valve prostheses. J Biomech 1986;19:39–51.
[35] Levesque MJ, Nerem RM. The elongation and orientation of cultured endothelial cells in response to shear stress. J Biomech Eng 1985;107:341–7.
[36] Bengtsson LA, Haegerstrand AN. Endothelialization of mechanical heart valves in vitro with cultured adult human cells. J Heart Valve Dis 1993;2:352–6.
[37] Garcia AJ, Gallant ND. Stick and grip: measurement systems and quantitative analyses of integrin-mediated cell adhesion strength. Cell Biochem Biophys 2003;39:61–73.
[38] Wojtowicz AM, Shekaran A, Oest ME, Dupont KM, Templeman KL, Hutmacher DW, et al. Coating of biomaterial scaffolds with the collagen-mimetic peptide GFOGER for bone defect repair. Biomaterials 2010;31:2574–82.
[39] Petrie TA, Capadona JR, Reyes CD, Garcia AJ. Integrin specificity and enhanced cellular activities associated with surfaces presenting a recombinant fibronectin fragment compared to RGD supports. Biomaterials 2006;27:5459–70.
[40] Gould RA, Butcher JT. Isolation of valvular endothelial cells. J Vis Exp Dec. 29 2010;46.
[41] Butcher JT, Penrod AM, Garcia AJ, Nerem RM. Unique morphology and focal adhesion development of valvular endothelial cells in static and fluid flow environments. Arterioscler Thromb Vasc Biol 2004;24:1429–34.
[42] Reyes CD, Petrie TA, Garcia AJ. Mixed extracellular matrix ligands synergistically modulate integrin adhesion and signaling. J Cell Physiol 2008;217:450–8.
[43] Reyes CD, Garcia AJ. Engineering integrin-specific surfaces with a triple-helical collagen-mimetic peptide. J Biomed Mater Res A 2003;65:511–23.
[44] Butcher JT, Nerem RM. Valvular endothelial cells regulate the phenotype of interstitial cells in co-culture: effects of steady shear stress. Tissue Eng 2006;12:905–15.
[45] Spinelli SL, Casey AE, Pollock SJ, Gertz JM, McMillan DH, Narasipura SD, et al. Platelets and megakaryocytes contain functional nuclear factor-kappaB. Arterioscler Thromb Vasc Biol 2010;30:591–8.
[46] Weston MW, LaBorde DV, Yoganathan AP. Estimation of the shear stress on the surface of an aortic valve leaflet. Ann Biomed Eng 1999;27:572–9.
[47] Yap CH, Saikrishnan N, Yoganathan AP. Experimental measurement of dynamic fluid shear stress on the ventricular surface of the aortic valve leaflet. Biomech Model Mechanobiol 2012;11:231–44.
[48] Barreto-Filho JA, Wang Y, Dodson JA, Desai MM, Sugeng L, Geirsson A, et al. Trends in aortic valve replacement for elderly patients in the United States, 1999–2011. J Am Med Assoc 2013;310:2078–85.
[49] Northrup 3rd WF, Dubois KA, Kshettry VR, Teskey JM, Nicoloff DM. Trends in aortic valve surgery in a large multi-surgeon, multi-hospital practice, 1979-1999. J Heart Valve Dis 2002;11:768–78 [discussion 78-9].
[50] Niclauss L, von Segesser LK, Ferrari E. Aortic biological valve prosthesis in patients younger than 65 years of age: transition to a flexible age limit? Interact Cardiovasc Thorac Surg 2013;16:501–7.
[51] David TE, David C, Woo A, Manlhiot C. The Ross procedure: outcomes at 20 years. J Thorac Cardiovasc Surg 2014;147:85–93.
[52] Zilla P, Brink J, Human P, Bezuidenhout D. Prosthetic heart valves: catering for the few. Biomaterials 2008;29:385–406.
[53] McIntosh CT, Warnock JN. Side-specific characterization of aortic valve endothelial cell adhesion molecules under cyclic strain. J Heart Valve Dis 2013;22:631–9.

[54] Chlupac J, Filova E, Havlikova J, Matejka R, Riedel T, Houska M, et al. The gene expression of human endothelial cells is modulated by sub-endothelial extracellular matrix proteins: short-term response to laminar shear stress. Tissue Eng Part A April 24 2014 [Epub ahead of print].
[55] Thoumine O, Nerem RM, Girard PR. Changes in organization and composition of the extracellular matrix underlying cultured endothelial cells exposed to laminar steady shear stress. Lab Invest 1995;73:565–76.
[56] Jang YH, Kwon CH, Kim SB, Selimovic S, Sim WY, Bae H, et al. Deep wells integrated with microfluidic valves for stable docking and storage of cells. Biotechnol J 2011;6:156–64.
[57] Polanowska-Grabowska R, Simon Jr CG, Gear AR. Platelet adhesion to collagen type I, collagen type IV, von Willebrand factor, fibronectin, laminin and fibrinogen: rapid kinetics under shear. Thromb Haemost 1999;81:118–23.
[58] Higuchi A, Sugiyama K, Yoon BO, Sakurai M, Hara M, Sumita M, et al. Serum protein adsorption and platelet adhesion on pluronic-adsorbed polysulfone membranes. Biomaterials 2003;24:3235–45.
[59] Tan A, Goh D, Farhatnia Y, Lim J, G N, Teoh SH, et al. An anti-CD34 antibody-functionalized clinical-grade POSS-PCU nanocomposite polymer for cardiovascular stent coating applications: a preliminary assessment of endothelial progenitor cell capture and hemocompatibility. PLoS One 2013;8:e77112.